J. Fluid Mech. (1993), *vol.* 249, *pp.* 227–239

Experimental study of two interacting drops in an immiscible fluid

By XIAOGUANG ZHANG, ROBERT H. DAVIS† AND MARK F. RUTH

Department of Chemical Engineering, University of Colorado, Boulder, CO 80309-0424, USA

(Received 2 July 1992 and in revised form 22 October 1992)

Experiments were performed in order to elucidate the effects of hydrodynamic interactions between two drops on their gravity-induced relative motion. The relative trajectories of two drops, their relative velocities, and the travel time for them to flow around each other were measured for different initial horizontal separations. Two size ratios and two viscosity ratios were investigated. Hydrodynamic interactions significantly reduce the relative velocity of two nearby drops and cause them to flow around each other with curved trajectories, resulting in a longer duration of the close encounter, compared with that for two non-interacting drops. These effects increase with decreasing drop separation, decreasing size ratio, and increasing viscosity ratio. Experimental results are in good agreement with theoretical predictions, except when the drops become sufficiently close that interface deformation occurs.

1. Introduction

Hydrodynamic interactions of drops with other drops dispersed in an immiscible fluid are of fundamental importance in a variety of natural and industrial processes, such as raindrop growth, liquid–liquid extraction, and the processing of liquid-phase miscibility gap and other composite materials. Under the action of gravity, drops of different sizes may approach each other due to their different settling velocities. When two drops are within several radii of each other, the presence of the neighbouring drop disturbs the velocity fields around each drop. These disturbances modify the velocity of each drop, with the effect increasing as the separation between the drops decreases. These hydrodynamic interactions resist the relative motion of the two drops and cause them to flow around each other. In this paper, we present the results of experimental studies on the hydrodynamic interactions between two drops undergoing gravity-induced relative motion.

Hydrodynamic interactions between two rigid or fluid spheres moving through a quiescent fluid at low Reynolds number have been studied extensively by theory (Jeffrey & Onishi 1984; Haber, Hetsroni & Solan, 1973; Zinchenko 1980). Previous efforts have focused on binary interactions of two spheres and yielded infinite series for the two-sphere resistance or mobility functions, which describe the hydrodynamic interactions between two spheres. Davis (1984) and Melik & Fogler (1984) used these functions in trajectory analyses to follow the gravity-induced relative motion of two rigid spheres. These analyses demonstrate the effects of hydrodynamic interactions on the trajectories of interacting particles, and they are especially useful in

† To whom correspondence should be addressed.

predicting collision rates. The trajectory analysis has recently been extended to predict the interactions and collisions between two spherical drops (Zhang & Davis 1991). In their study, the role of the internal flow within the drops, which becomes more important with decreasing viscosity of the drop phase compared with that of the matrix fluid, was addressed.

In contrast to intensive theoretical efforts on hydrodynamic interactions of two spheres, experimental studies of the subject are relatively sparse. Experimental investigations of hydrodynamic interactions of two rigid spheres in low-Reynolds-number simple shear flow were performed by Arp & Mason (1977) for equal-sized spheres and by Adler (1981) for unequal-sized spheres. Considerable data for the relative trajectories of two spheres, the relative velocity of two non-touching spheres, and the rolling velocity of two touching spheres were obtained, and they show good agreement with theoretical prediction (except when the particles are so close that small surface roughness affects their interaction). However, fluid drops behave differently in regard to hydrodynamic interactions, primarily because of internal flow and interface deformation. In particular, the internal flow, which may be described in terms of an interface mobility, allows two drops to approach each other with less hydrodynamic resistance than for rigid spheres (Davis, Schonberg & Rallison 1989), whereas interface deformation significantly reduces the relative velocity between the two drops (Yiantsios & Davis 1991). Unfortunately, experimental data for the interaction of two fluid drops under low-Reynolds-number flow conditions are limited. A series of experiments on the interaction of a settling drop and a planar surface under the action of gravity were carried out by Bart (1968). The experimental results for the terminal settling velocity of the drop as a function of its distance from the surface suggest a qualified support of theory. Recently, Barton & Subramanian (1990) performed experiments to investigate the effects of hydrodynamic interactions of a fluid drop and a solid planar surface on drop migration driven by gravity, by predominately thermocapillary effects, and by comparable gravity and thermocapillary effects which are aligned in opposite directions. In all three cases, the experimentally measured drop velocities are in excellent agreement with theoretical predictions. Similar experiments on gas bubbles have been conducted by Merritt & Subramanian (1989).

Although extensive studies have been made on the impact of two drops at high velocities (Brazier-Smith, Jennings & Latham 1972; Ashgriz & Poo 1990; Jiang, Umemura & Law 1992), experimental results for hydrodynamic interactions between two drops in low-Reynolds-number flow are rare. An exception is the investigation by Bartok & Mason (1959) on the approach, rotation, and separation or coalescence of two drops in simple shear. The current study involves experiments to test the theory for low-Reynolds-number interactions during gravity-induced relative motion of two small drops. In this paper, details of the experimental materials and methods are described in §2. In §3, we provide the necessary theoretical results extracted from Zhang & Davis (1991). Section 4 presents the experimental results and their comparison with theory. Concluding comments are provided in §5.

2. Experimental materials and methods

A schematic of the experimental apparatus is shown in figure 1. The glass chamber has dimensions 8×8 cm in the horizontal cross-section, and is 25 cm in depth. This size is sufficiently large that wall effects are negligible, and it allows for the two drops to start with a large vertical separation. The chamber is immersed in a large water

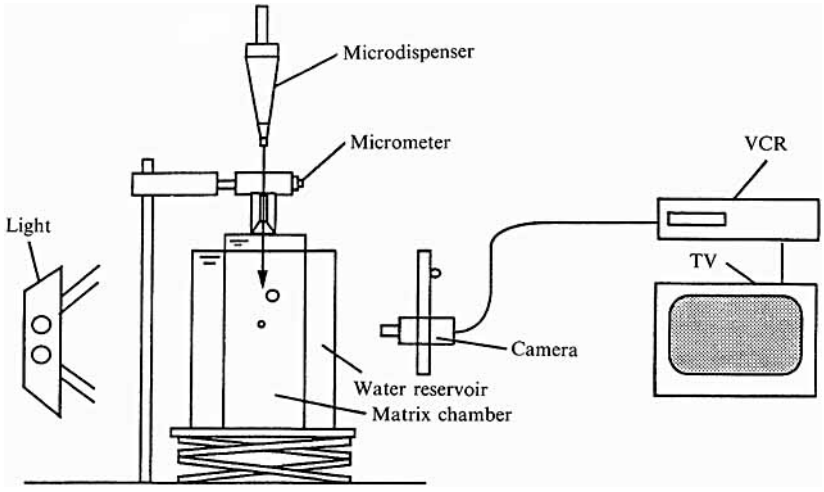

FIGURE 1. Sketch of the experimental setup for gravity-induced motion of two drops.

reservoir to keep the temperature of the fluids constant. Inside the chamber, a mirror standing vertically is positioned at a 45° angle from the view of a Sanyo VDC 3860 video camera. This mirror is visible to the camera, allowing the drops to be viewed from two perpendicular angles simultaneously. Observing the two views makes it possible to accurately measure both the horizontal and the vertical separation between the drops. The camera is held on a focusing rail so that it can be manually moved to follow drops, and it is connected to a Panasonic AG-1830 video cassette recorder and a Panasonic CT-2010Y colour video monitor to observe and record the drop motion.

Drops were introduced in the top of the chamber by inserting a microdispenser filled with the drop fluid into the matrix and releasing a certain amount of the fluid to form a drop. By adjusting the volume of the released fluid, the drop size can be controlled. Under the accuracy limits for the delivery volume of the microdispenser, the smallest drop generated for the present experiments was 0.35 mm in radius. The microdispenser is placed into position by inserting it through a hole bored in a specially designed holder. Mounted on a micrometer with a precision of 0.01 mm, this holder can have its position changed horizontally in the direction perpendicular to the view of the camera; therefore, the initial horizontal positions of drops can be adjusted.

Two fully immiscible fluid systems having different viscosity ratios were chosen. One system consists of castor oil (drops) in the GE silicone fluid SF-1147 (matrix) with a viscosity ratio of 13.3. The system chosen for a low viscosity ratio of 0.76 is the Union Carbide fluid UCON 50HB-280X (drops) in heavy paraffin oil (matrix). The relevant properties of these fluids are listed in table 1, where μ' and μ are viscosities of the drop phase and the matrix fluid, respectively, ρ' and ρ are their densities, γ is the interfacial tension, and $U_1^{(0)}$ represents the settling velocity of an isolated drop with radius a_1.

Because of small density differences of the drop phases and the matrix fluids, and the high viscosities of the chosen matrix fluids, the gravity-induced settling velocity of an isolated drop is sufficiently small that the Reynolds numbers, $Re = \rho a_1 U_1^{(0)}/\mu$, for the two systems are much smaller than unity (table 1). Therefore, inertial effects upon the drops are negligible when compared to viscous effects. In addition, the

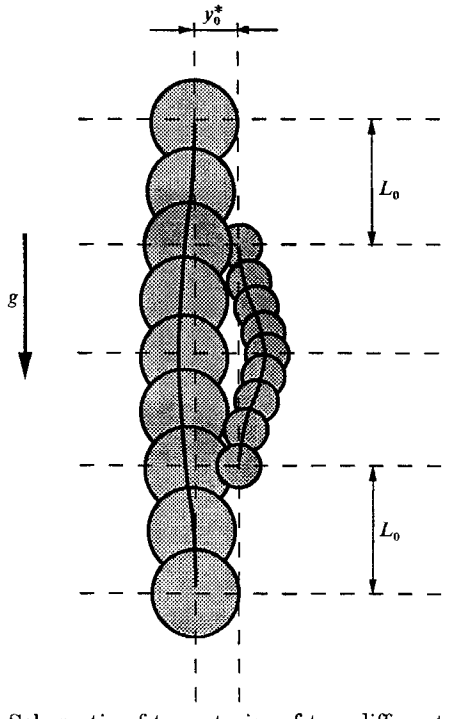

FIGURE 2. Schematic of trajectories of two different-sized drops.

	μ'/μ (g/cm s)	ρ'/ρ (g/cm^3)	γ (dyn/cm)	$U_1^{(0)}$ (mm/s)	*Re*	*Ca*
Castor oil–GE fluid	6.87/0.52	0.959/0.888	2.29	2.22	0.030	0.050
UCON fluid–paraffin oil	1.33/1.76	1.034/0.880	4.93	1.55	0.0063	0.055

TABLE 1. Properties of fluids used in experiments at 22.5°, where the velocity, Reynolds number, and Capillary number shown are based on a larger drop radius of 0.8 mm

capillary number, $Ca = \mu U_1^{(0)}/\gamma$, provides a measure of the relative importance of viscous effects and capillary effects. As described by Yiantsios & Davis (1991), deformation is expected to become important when the separation between the interfaces of the two drops, h_0, becomes comparable to $a_2 Ca$, where a_2 is the radius of the smaller drop. From table 1, it is then apparent that deformation will be significant when the separation distance is approximately 5% of the smaller drop radius.

When performing each experiment, the smaller drop was introduced first and allowed to settle through part of the chamber. After the first drop had settled a certain distance, a second, larger drop was inserted and allowed to settle towards the first one. Being larger, the second drop settled faster than the first one, leading to the two drops approaching, passing around, and separating from each other, as shown schematically in figure 2. The entire process of introduction, approach, interaction, and separation of the two drops was magnified and videotaped. The taped video was then reviewed and analysed. As described in §4, the velocities of individual drops when isolated were measured and compared to theory first in order to check for convective and interfacial effects.

3. Theory

A theoretical analysis for the hydrodynamic interaction of two fluid drops undergoing gravitational sedimentation has been presented previously (Zhang & Davis 1991). In the following, the salient features of the theory are described and arranged in forms that may be compared with the experiments, with most of the mathematical details omitted.

The analysis is restricted to binary interactions of two drops with radii a_1 and a_2, which are arbitrarily oriented, as shown in figure 3. The two drops are composed of the same material and are assumed to remain spherical. The motion of the drops occurs at a Reynolds number much smaller than unity, and so inertial effects are negligible when compared with viscous effects. Under these assumptions, the velocity $\boldsymbol{V}_{12}$ of drop 1 relative to drop 2 is linearly related to the gravitational force and depends only on the instantaneous relative position of the two drops. An expression for this relative velocity has been presented by Batchelor (1982):

$$\boldsymbol{V}_{12}(\boldsymbol{r}) = \boldsymbol{V}_{12}^{(0)} \cdot \left[\frac{\boldsymbol{rr}}{r^2} L(s) + \left(\boldsymbol{I} - \frac{\boldsymbol{rr}}{r^2}\right) M(s)\right], \tag{1}$$

where $\boldsymbol{r}$ is the vector from the centre of drop 1 to the centre of drop 2 and $\boldsymbol{I}$ is the unit second-order tensor. The relative velocity of two isolated non-interacting drops due to gravity is given by the Hadamard-Rybczynski formula:

$$\boldsymbol{V}_{12}^{(0)} \equiv \boldsymbol{U}_2^{(0)} - \boldsymbol{U}_1^{(0)} = \frac{2(\hat{\mu}+1)(\rho'-\rho)a_1^2(\lambda^2-1)\boldsymbol{g}}{3(3\hat{\mu}+2)\mu}, \tag{2}$$

where $\hat{\mu} = \mu'/\mu$ is the viscosity ratio, $\lambda = a_2/a_1$ is the size ratio, and $\boldsymbol{g}$ is the local gravitational acceleration vector. The relative mobility functions L and M are the hydrodynamic correction factors for the gravity-induced relative motion along and normal to the line of centres, respectively, in order to describe the effects of hydrodynamic interactions. Each of these functions depends on the size ratio, the viscosity ratio, and the dimensionless separation between drops: $s = 2r/(a_1+a_2)$, where $r = |\boldsymbol{r}|$ is the centre-to-centre spacing. They are equal to unity for $s \to \infty$, and decrease with s decreasing.

For two arbitrarily separated drops, solutions for the hydrodynamic interactions – based on the method of bispherical coordinates – have been developed by Haber *et al.* (1973) for the motion along their line of centres and by Zinchenko (1980) for the motion perpendicular to the line of centres. Moreover, asymptotic expansions for widely separated and near-contact drops have been derived by Hetsroni & Haber (1978) and Davis *et al.* (1989), using the method of reflections and lubrication theory, respectively. These solutions show that hydrodynamic interactions significantly reduce the relative motion of two drops, particularly for the motion along the line of centres. Comprehensive information on the relative mobility functions for various size ratios and viscosity ratios is presented by Zhang & Davis (1991).

Decomposing the relative velocity given by (1) into its components along and perpendicular to the line of centres (i.e. in the radial and tangential directions, as shown in figure 3) yields

$$V_{r,12} = \mathrm{d}r/\mathrm{d}t = -V_{12}^{(0)} L \cos\theta, \tag{3}$$

$$V_{\theta,12} = r(\mathrm{d}\theta/\mathrm{d}t) = V_{12}^{(0)} M \sin\theta, \tag{4}$$

where $V_{12}^{(0)} = |\boldsymbol{V}_{12}^{(0)}|$ is the magnitude of relative velocity of two non-interacting drops,

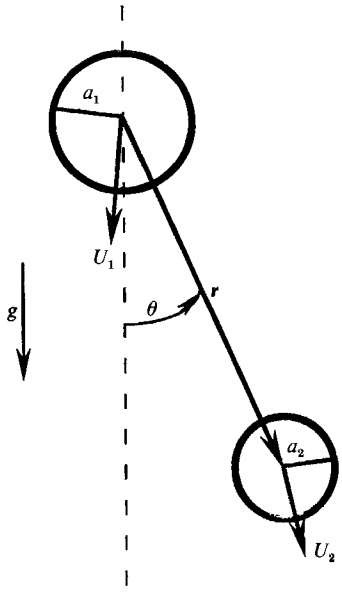

FIGURE 3. Sketch of two spherical drops moving with arbitrary orientation under the action of gravity.

and θ is the angle between the line of centres and the gravity vector. Dividing the radial by the tangential component and converting to $s = 2r/(a_1+a_2)$, we obtain the dimensionless relative trajectory equation:

$$\frac{\mathrm{d}s}{\mathrm{d}\theta} = -s\frac{L(s)\cos\theta}{M(s)\sin\theta}. \tag{5}$$

By integrating this equation subject to an initial configuration, we can predict the relative trajectory of two interacting drops. The interaction time for the two drops to flow around each other, and their instantaneous relative velocity, may then be found from (3) and (4).

4. Results and discussion

The experimental trials started with testing a single drop settling individually in the matrix fluid and comparing its settling velocity with theory. Since the volume released by the microdispenser was not exact, the radii of the drops created in the experiments deviated slightly from the controlled values. The drop sizes measured from the videotape and averaged for all 20 experiments are listed in table 2 for the two systems, along with plus and minus one standard deviation of the drop radii. Besides the uncertainty of the released volume of the drop fluid, the deviation of the drop sizes may also result from measurement errors. At camera and VCR zoom magnifications, totalling 46.8×, the drop radii were measured to a precision of ± 0.02 mm. The measured settling velocities of different isolated drops and those calculated by the Hadamard–Rybczynski formula, (2), using the measured drop radii are also presented in table 2. The results show reasonable agreement between experiments and theory. However, the standard deviations of the measured velocities are larger than theoretical ones, particularly for the smaller drops. The standard deviations listed for the experiments are those determined from the actual

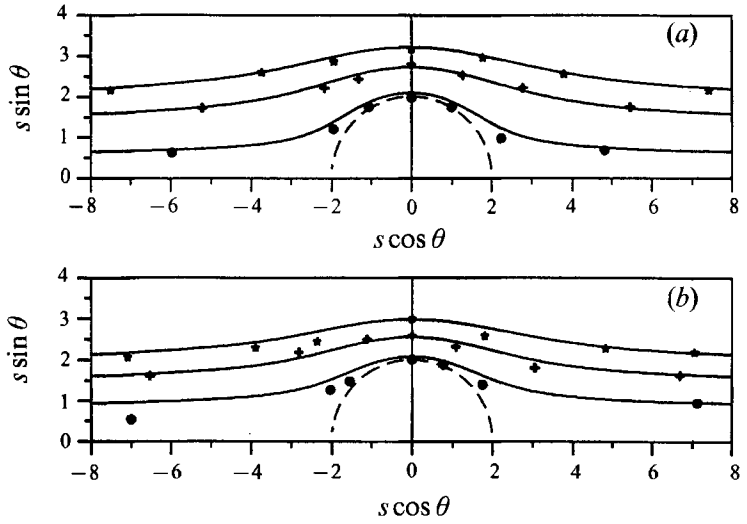

FIGURE 4. Relative trajectories of two interacting drops with $\lambda = 0.5$ and different initial horizontal separations: (*a*) for the castor oil–GE fluid system with $\hat{\mu} = 13.3$; (*b*) for the UCON fluid–paraffin oil system with $\hat{\mu} = 0.76$. The solid lines are theoretical predictions and the relative motion is from right to left.

			$U_1^{(0)}$ (mm/s)		$U_2^{(0)}$ (mm/s)	
	a_1 (mm)	a_2 (mm)	experiment	theory	experiment	theory
Castor oil–GE fluid	0.79±0.02	0.39±0.01	2.07±0.14	1.90±0.07	0.48±0.06	0.46±0.02
UCON fluid–paraffin oil	0.84±0.02	0.42±0.01	1.57±0.09	1.65±0.08	0.39±0.05	0.41±0.02

TABLE 2. Average drop radii and isolated settling velocities

measurements of the falling speeds, whereas those listed for the theory are calculated from the measured variation in drop sizes. A possible factor which would contribute to this discrepancy between experiment and theory is convection inside the matrix fluid. A small amount of uncertain, background motion within the matrix fluid aggravates the deviation of the measured velocities, and its effects become significant for the smaller drops whose settling velocities are not much greater in magnitude than the background convection. As a consequence of the convection, it was found in experiments that the drops wandered slightly in the horizontal direction as well.

Experiments were conducted with two different-sized drops being released with different initial horizontal separations. As predicted, the smaller the initial horizontal distance is, the smaller the separation between the drops will become as they flow around each other; therefore, the drops will experience a stronger hydrodynamic resistance, resulting in a slower relative velocity and more deviation from the rectilinear trajectories. The curved relative trajectories of two drops which start with different initial horizontal separations are shown in figure 4 for the two systems with a size ratio of $\lambda = a_2/a_1 = 0.5$. In this figure, the solid lines represent the theoretical predictions determined by numerically integrating (5), and the points are experimental results. Relatively good agreement between the results is demon-

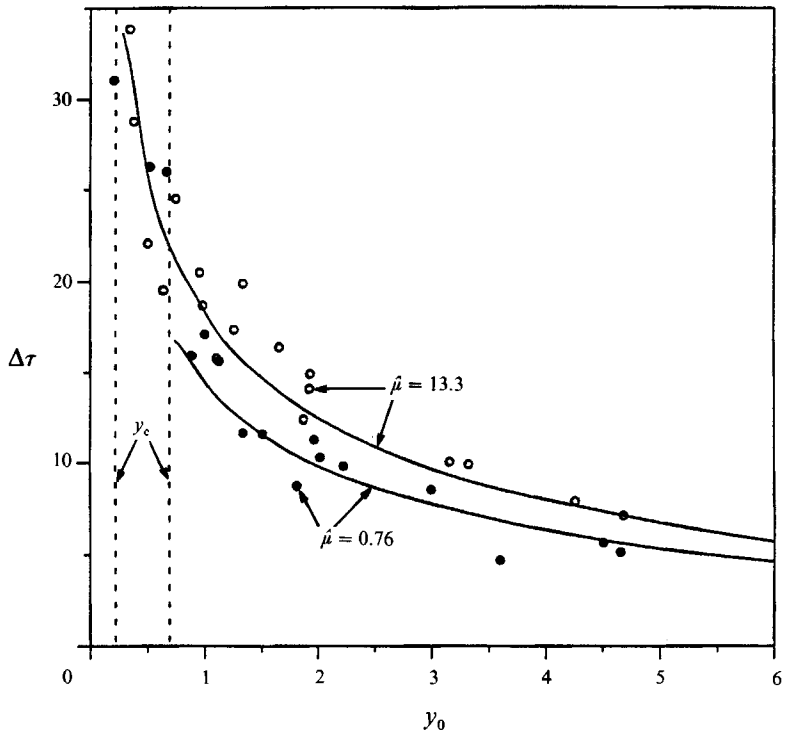

FIGURE 5. Differential travel time for two drops with $\lambda = 0.5$ due to hydrodynamic interactions versus the initial horizontal separation; the solid lines are theoretical predictions.

strated, except for when the two drops are very close to one another, where interface deformation allows the two drops to move closer than predicted for spherical drops. Moreover, at a camera magnification, 16.3×, the measurement uncertainty in the distance between the two drop centres was ± 0.15 mm, which is more than 10% of the centre-to-centre distance when the two drops are very close to one another.

The hydrodynamic interactions resist the relative motion of two drops, and force the drops to flow around each other with curved trajectories instead of rectilinear trajectories. Therefore, a longer time is required for the larger drop to pass around the smaller one than in the absence of interactions. The travel time was measured for the two drops to pass around each other from a prescribed initial vertical separation, L_0, to an equal final vertical separation, as shown in figure 2. In analysing our experiments, the dimensionless value of this separation was chosen to be $H_0 = 2L_0/(a_1+a_2) = 14.0$. The distance and time measurements were made possible because vertical reference lines were videotaped behind the drops. The results for the dimensionless difference $\Delta\tau = 2(t-t^{(0)})\, V_{12}^{(0)}/(a_1+a_2)$ between the measured time, t, for the two interacting drops to move from a dimensionless vertical separation of $+H_0$ to one of $-H_0$, and that predicted for two non-interacting drops, $t^{(0)}$, are presented in figure 5. By subtracting the time for two non-interacting drops to move the same distance, the effects of hydrodynamic interactions are more definitely described by the additional time required for the drops to overcome the hydrodynamic resistance. The experimental results show good agreement with the theoretical predictions, although there is moderate scatter in the data due to

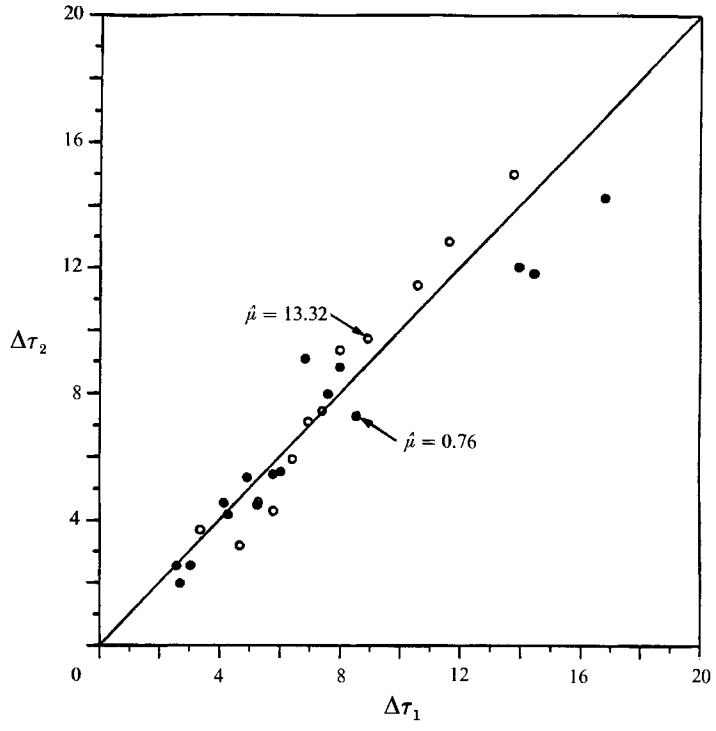

FIGURE 6. Differential travel times for two drops in the approach half of their trajectories, $\Delta\tau_1$, versus those in the receding half, $\Delta\tau_2$, for $\lambda = 0.5$; the 45° solid line is the theoretical prediction.

convection and measurement uncertainties. For large values of the dimensionless initial horizontal separation, $y_0 = 2y_0^*/(a_1+a_2)$, $\Delta\tau \to 0$ because the hydrodynamic interactions are negligible. With decreasing initial horizontal separation, the differential or delay time increases due to increasing hydrodynamic interactions.

When the initial horizontal separation is smaller than a critical value, $y_0 < y_c$, two spherical drops are predicted to collide and coalesce with each other (Zhang & Davis 1991). For the system with $\hat{\mu} = 0.76$ and $\lambda = 0.5$, the critical value is $y_c = 0.67$, whereas it is $y_c = 0.20$ for the system with $\hat{\mu} = 13.3$ and $\lambda = 0.5$. However, collisions of the two drops were rarely observed, even when the initial horizontal separation was smaller than the critical value, presumable due to deformation of the drops caused by lubrication forces when in near contact. The deformation significantly reduces the drop relative velocity, and its effects increase with decreasing distance between the two drops. The three data points in figure 5 with $y_0 < y_c$ for $\hat{\mu} = 0.76$ confirm this by showing a large interaction time but no coalescence. Finally, we note that drops with a large viscosity ratio experience stronger hydrodynamic resistance to their relative motion than do drops with a small viscosity ratio, and so it takes a longer time for the larger drop to pass around the smaller one. This trend is confirmed by the experimental data of figure 5.

In the absence of colloidal effects, the trajectories of two spherical drops are predicted to be symmetric with respect to the plane in which $\theta = \frac{1}{2}\pi$. In order to check this symmetry, the measured differential times for two drops during the approach and receding halves of their trajectories were compared with each other and are shown in figure 6. The theoretical prediction of a 45° straight line is presented as a reference. It is clear that most of the experimental results are in reasonable

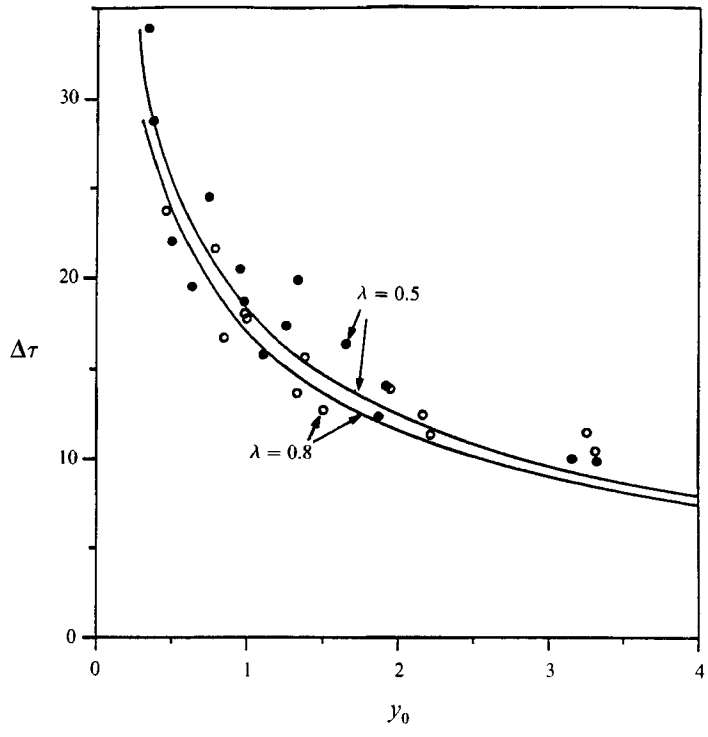

FIGURE 7. Differential travel time due to hydrodynamic interactions for the castor oil–GE fluid system with $\hat{\mu} = 13.3$ for different size ratios versus the initial horizontal separation; the solid lines are theoretical predictions.

agreement with the theory, except for some scatter which probably resulted from small measurement uncertainties and convection inside the matrix fluid. However, for the drops with $\hat{\mu} = 0.76$ and $y_0 < y_c$ (corresponding to the three solid circles furthest to the right in figure 6), the differential time spent in the approach half of the drop trajectories is about 20% longer than that in the receding half. Although the difference is not significant at the 95% confidence level, it is consistent with the expectation that deformation would break the symmetry of the drop trajectories.

Figure 7 presents results of the differential time with different size ratios, $\lambda = 0.5$ and 0.8, for the castor oil–GE fluid system with $\hat{\mu} = 13.3$. The theory predicts that, with decreasing size ratio, the smaller drop tends to follow along the fluid streamlines surrounding the larger drop, and is easily displaced by the larger drop, resulting in a more curved relative trajectory of the two drops and a longer time for the two drops to flow around each other. However, the difference between the predicted results for the two size ratios employed is small, and the scatter in the experimental data is too great for the difference in the time to be clearly detected.

The experimental results were also analysed to determine the relative mobility functions, L and M. The distance between two drops, r, and the angle between the line of centres of the drops and the gravity vector, θ, were measured at set time separations. After non-dimensionalizing the distances and the time, the variations of the distance and the angle with time were determined by best fitting the measured values with polynomials using the method of least squares in the region between $s = 10.0$ and 2.4. By differentiating these best fits of the data with respect to time,

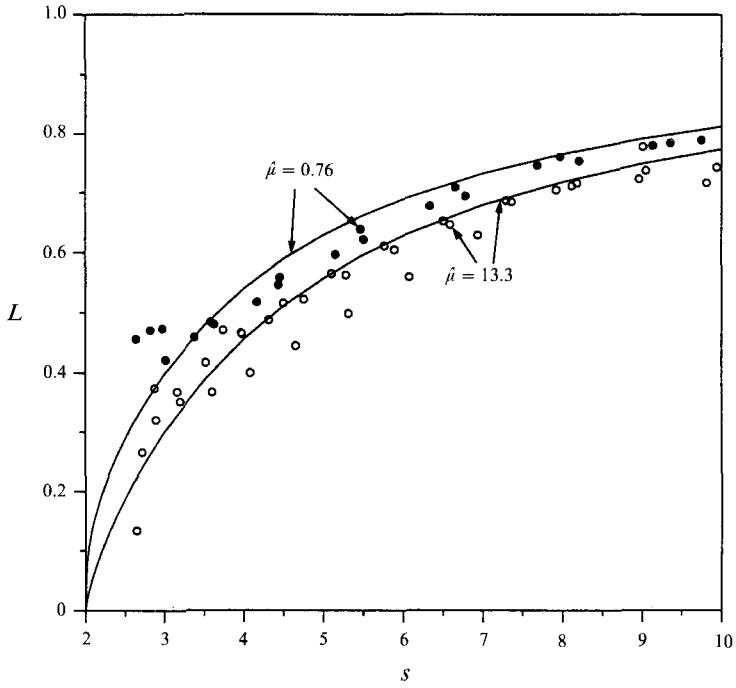

FIGURE 8. The relative mobility function for two drops with $\lambda = 0.5$ moving along the line of centres versus the dimensionless separation distance; the solid lines are theoretical predictions.

the relative mobility functions along and normal to the line of centres were determined from the dimensionless forms of (3) and (4), respectively:

$$L = -\frac{\mathrm{d}s/\mathrm{d}\tau}{\cos\theta}, \tag{6}$$

$$M = \frac{s\mathrm{d}\theta/\mathrm{d}\tau}{\sin\theta}, \tag{7}$$

where $\tau = 2V_{12}^{(0)}t/(a_1+a_2)$ is the dimensionless time.

The relative mobility functions were determined from three experiments for each system, and the results are plotted in figures 8 and 9, for motion along and normal to the line of centres, respectively. Data for which $\cos\theta < 0.1$ or $\sin\theta < 0.1$ were not included in the determination of L or M, respectively, because small measurement errors would then cause large errors in the computed mobility functions. For comparison, the corresponding theoretical results from the exact solutions by the method of bispherical coordinates (Haber *et al.* 1973; Zinchenko 1980) are presented in figures 8 and 9 as solid lines. Given the uncertainty in the measurements and the error propagation due to differentiation of experimental data, these figures show good agreement between experiment and theory. For the larger viscosity ratio, the relative velocity between the two drops is lower due to larger hydrodynamic interactions, and this is indicated by the decreasing relative mobility functions. Moreover, the relative mobility functions decrease with decreasing separation between the two drops, due to increasing hydrodynamic interactions. Hydrodynamic interactions offer greater resistance to the motion along the line of centres and cause its relative mobility function to tend toward zero as the two drops come into physical contact ($s \to 2$).

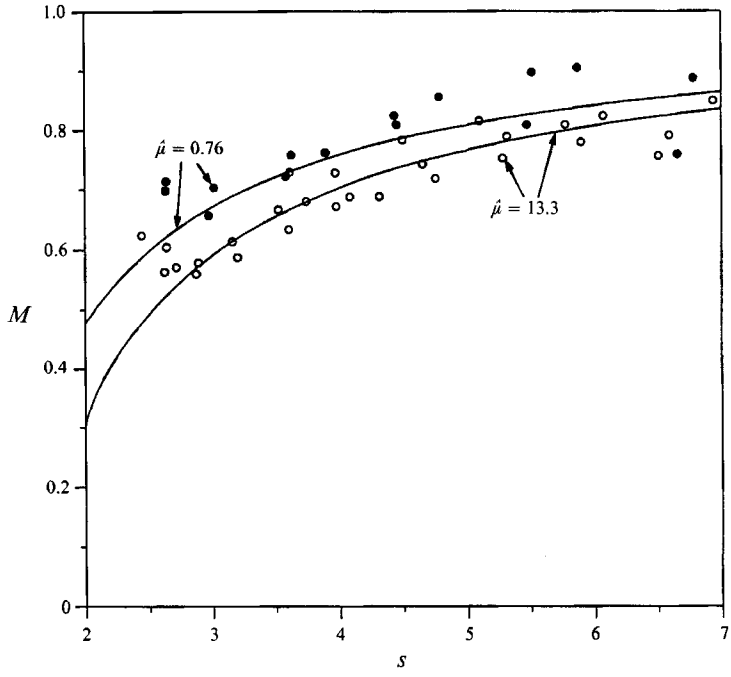

FIGURE 9. The relative mobility function for two drops with $\lambda = 0.5$ moving normal to the line of centres versus the dimensionless separation distance; the solid lines are theoretical predictions.

5. Concluding remarks

Effects of hydrodynamic interactions on gravity-induced relative motion of two drops were determined experimentally. These effects were analysed in terms of the relative trajectories, the relative mobility functions, and travel time for the drops to move past each other. Most of the experimental results were found to be in good agreement with theoretical predictions, except when the drops became so close that deformation was expected to occur due to lubrication forces in the gap between them. Employing smaller drops would reduce the effects of deformation, although this would require more sophisticated equipment for producing the drops, reducing convection, and providing sufficient magnification.

Experimental results demonstrate that hydrodynamic interactions significantly reduce the relative velocity of two nearby drops and cause the two drops to flow around each other with curved trajectories, resulting in a longer time for the two drops to pass around each other. Moreover, the theoretical predictions that the effects of hydrodynamic interactions increase as the drop separation decreases, the size ratio decreases, and the viscosity ratio increases are also confirmed.

This paper is based upon work supported by NSF Grant CTS-8914236 and NASA Grants NAG3-993 and NAG3-1277.

REFERENCES

ADLER, P. M. 1981 Interaction of unequal spheres. III. Experimental. *J. Colloid Interface Sci.* **84**, 489–496.

ARP, P. A. & MASON, S. G. 1977 The kinetics of flowing dispersions. IX. Doublets of rigid spheres (Experimental). *J. Colloid Interface Sci.* **61**, 44–61.

ASHGRIZ, N. & POO, J. Y. 1990 Coalescence and separation in binary collisions of liquid drops. *J. Fluid Mech.* **221**, 183–204.

BART, E. 1968 The slow unsteady settling of a fluid sphere toward a flat fluid interface. *Chem. Engng Sci.* **23**, 193–210.

BARTOK, W. & MASON, S. G. 1959 Particle motions in sheared suspensions. VIII. Singlets and doublets of fluid spheres. *J. Colloid Sci.* **14**, 13–26.

BARTON, K. D. & SUBRAMANIAN, R. S. 1990 Thermocapillary migration of a liquid drop normal to a plane surface. *J. Colloid Interface Sci.* **137**, 170–182.

BATCHELOR, G. K. 1982 Sedimentation in a dilute polydisperse system of interacting spheres. *J. Fluid Mech.* **119**, 379–408.

BRAZIER-SMITH, P. R., JENNINGS, S. G. & LATHAM, J. 1972 The interaction of falling water drops: coalescence. *Proc. R. Soc. Lond.* A **326**, 393–408.

DAVIS, R. H. 1984 The rate of coagulation of a dilute polydisperse system of sedimenting spheres. *J. Fluid Mech.* **145**, 179–199.

DAVIS, R. H., SCHONBERG, J. A. & RALLISON, J. M. 1989 The lubrication force between two viscous drops. *Phys. Fluids* A **1**, 77–81.

HABER, S., HETSRONI, G. & SOLAN, A. 1973 On the low Reynolds number motion of two droplets. *Intl J. Multiphase Flow* **1**, 57–71.

HETSRONI, G. & HABER, S. 1978 Low Reynolds number motion of two drops submerged in a unbounded arbitrary velocity field. *Intl J. Multiphase Flow* **4**, 1–17.

JEFFREY, D. J. & ONISHI, Y. 1984 Calculations of the resistance and mobility functions for two unequal rigid spheres in low-Reynolds-number flow. *J. Fluid Mech.* **139**, 261–290.

JIANG, Y. J., UMEMURA, A. & LAW, C. K. 1992 An experimental investigation on the collision behavior of hydrocarbon droplets. *J. Fluid Mech.* **234**, 171–190.

MELIK, D. H. & FOGLER, H. S. 1984 Gravity-induced flocculation. *J. Colloid Interface Sci.* **101**, 72–83.

MERRITT, R. M. & SUBRAMANIAN, R. S. (1989) Migration of a gas bubble normal to a plane horizontal surface in a vertical temperature gradient. *J. Colloid Interface Sci.* **131**, 514–525.

YIANTSIOS, S. G. & DAVIS, R. H. 1991 Close approach and deformation of two viscous drops due to gravity and van der Waals forces. *J. Colloid Interface Sci.* **144**, 412–433.

ZHANG, X. & DAVIS, R. H. 1991 The rate of collisions due to Brownian or gravitational motion of small drops. *J. Fluid Mech.* **230**, 479–504.

ZINCHENKO, A. Z. 1980 The slow asymmetric motion of two drops in a viscous medium. *Prikl. Mat. Mech.* **44**, 30–37.